JOURNAL OF SPACECRAFT AND ROCKETS
Vol. 31, No. 2, March–April 1994

Simplified Model for Calculation of Backflow Contamination from Rocket Exhausts in Vacuum

Rhonald M. Jenkins,* Alessandro Ciucci,† and John E. Cochran Jr.‡
Auburn University, Auburn, Alabama 36849

A computationally simple procedure for estimating the backflow from a plume expanding into a vacuum has been developed. The continuum flow is modeled as in the Simons method, with straight streamlines radiating from a point on the plume axis of symmetry, constant velocity, and density varying inversely as the square of the radius. The continuous transition from continuum to free-molecular flow is replaced by a suitably defined discontinuity surface. Particle number densities outside the discontinuity surface are calculated by assuming that a Maxwellian velocity distribution exists for particles located within small volumes adjacent to that surface. The boundary layer at the nozzle exit is accounted for and may be large compared with the freestream inviscid flow region. Calculated results are compared with existing backflow data for nozzles using CO_2 as a propellant.

Nomenclature

A_e = nozzle exit area
A^* = nozzle throat area
C = parameter defined by Eq. (7)
d = molecular collision cross section
$d\sigma$ = area associated with elemental volume $d\tau$
$d\tau$ = elemental volume located on discontinuity surface
$d\Omega$ = element of solid angle of $d\tau$ as seen from an arbitrary point in space
K = plume normalization constant
K_n = Knudsen number
$\bar{L}$ = line of sight vector
M_e = nozzle exit Mach number
MW = gas molecular weight
N_A = Avagadro's number
$\hat{n}$ = unit vector normal to discontinuity surface at $d\tau$
n_τ = particle number density in $d\tau$
n_p = particle number density at an arbitrary point in space
P = Bird's "breakdown" parameter, defined by Eq. (9)
R_e = nozzle exit radius
r = radial coordinate
$\bar{r}$ = position vector from origin to $d\tau$
$\hat{r}$ = unit vector along $\bar{r}$
S = distance along streamlines
U_ℓ = limiting velocity of the inviscid core gas
$\bar{U}_\ell$ = average limiting velocity of the boundary-layer gas
u = flow velocity
$\bar{u}$ = u normalized with respect to most probable thermal velocity
x, y, z = Cartesian coordinates
α = u/U_ℓ
β = boundary-layer parameter, defined by Eq. (6)
δ = boundary-layer thickness
γ = ratio of specific heats
θ_0 = limiting turning angle for inviscid core flow
θ_∞ = limiting turning angle for nozzle flow, based on nozzle exit Mach number
ν = molecular collision frequency
ρ = density
ϕ, θ = angular coordinates
ψ = included angle between $\bar{u}$ and $\bar{L}$

Received June 23, 1990; presented as Paper 90-1846 at the AIAA/SAE/ASME/ASEE 26th Joint Propulsion Conference, Orlando, FL, July 16–18, 1990; revision received July 6, 1991; accepted for publication Nov. 2, 1992.

*Assistant Professor, Aerospace Engineering. Senior Member AIAA.
†Graduate Research Assistant, Aerospace Engineering. Student Member AIAA.
‡Professor, Aerospace Engineering. Associate Fellow AIAA.

Introduction

THE problem of spacecraft contamination, significant since the beginning of space exploration, is becoming increasingly important with the advent of sophisticated satellite systems and long-term missions such as the Space Station. A primary source of contamination is the exhaust flow from thrusters aboard the spacecraft. Because of the very low ambient pressure, portions of the exhaust may turn through large angles, and impingement on surfaces upstream of the thruster exit plane may occur.

Contamination, expressed by mass deposition and environmental degradation, is generally related to both forward flow and backward flow plume effects. As used here, backward flow refers to the portion of the exhaust turning at angles beyond those predicted by continuum theory. Prediction of the backflow is complicated by the interaction of the nozzle wall boundary layer with the inviscid core flow at the expansion corner of the nozzle lip. In addition, the very low ambient pressure implies that the overall plume flowfield will be divided into three distinct regimes: continuum, transition, and free molecular.

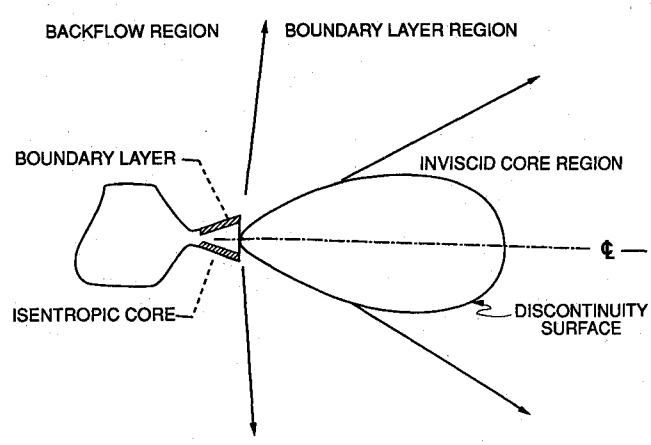

Fig. 1 Basic plume structure for model.

Methods traditionally used in the prediction of the properties of the expanding plume include the Simons model,[1] the method of characteristics (MOC),[2] and the direct simulation Monte Carlo (DSMC)[3] method. The Simons model is, by far, the simplest and least computationally complex analysis; the method of characteristics, combined with boundary-layer models, is used in existing computer codes such as CONTAM.[2] Both of these techniques are based on continuum equations, however, and are not suited for calculation of flows in the transition and free-molecular regimes. The DSMC method is perfectly suited for such calculations, but at the expense of very large computational times. Boyd and Stark[4] have analyzed a small hydrazine monopropellant thruster using all three methods. The choice of method generally involves a tradeoff between the degree of accuracy desired and the computational costs incurred.

The present work is based on the premise that it is useful and instructive to achieve reasonably accurate results in as timely a manner as possible, especially in the area of parametric investigation. The analysis proceeds from the Simons method as modified by Zana and Hoffman[5], to account for relatively large nozzle exit boundary layers. Then, following Noller[6] and, later, Grier,[7] the continuous transition from continuum to free-molecular flow is replaced by a suitably defined discontinuity surface; particle number densities outside the discontinuity surface are then calculated by assuming that a Maxwellian velocity distribution exists for particles located within small volumes adjacent to that surface. The discontinuity surface itself may be either a constant Knudsen number surface or a surface defined by a "breakdown parameter" as defined by Bird[8]; within the limitations of the present analysis, the two are equivalent. It should be noted that the present analysis differs from that of Grier[7] in that boundary-layer effects are accounted for in the model presented here.

Analysis

The Simons method is a source flow analysis, valid in the far field where the flow behaves as if it were diverging radially from a point source. In addition, the flow in the far field is assumed to have nearly reached its adiabatic limiting speed. Consequently, continuity requires that the local density, $\rho(r, \theta)$, varies inversely as the square of the distance from the source. Simons' equation is

$$\frac{\rho(r,\theta)}{\rho^*} = K\left(\frac{R^*}{r}\right)^2 f(\theta) \tag{1}$$

where K, the "plume normalization constant," is determined from continuity considerations and * refers to conditions at the nozzle throat. The function $f(\theta)$ relates the local density $\rho(r, \theta)$ to the plume centerline density and is given by

$$f(\theta) = \left[\cos\left(\frac{\pi}{2}\frac{\theta}{\theta_\infty}\right)\right]^{\frac{2}{\gamma-1}} \qquad \text{for} \qquad 0 \le \theta \le \theta_0 \tag{2}$$

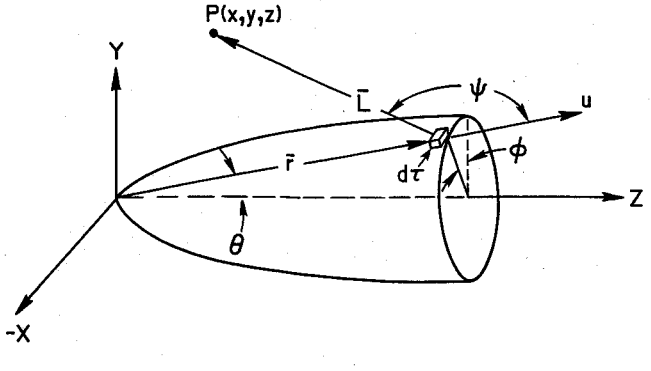

Fig. 2 Model geometry.

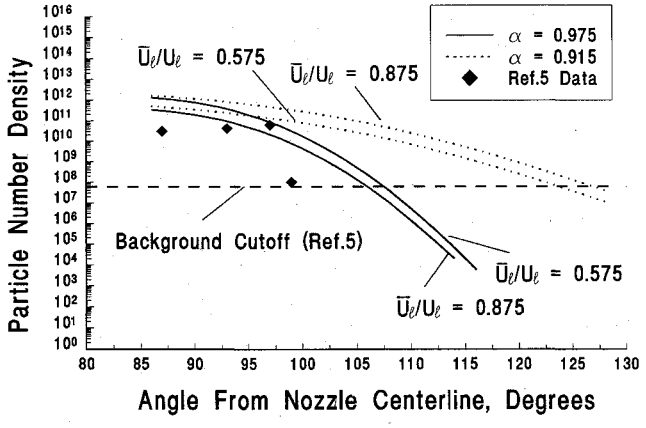

Fig. 3 Particle number density distributions for Ref. 5 nozzle geometry.

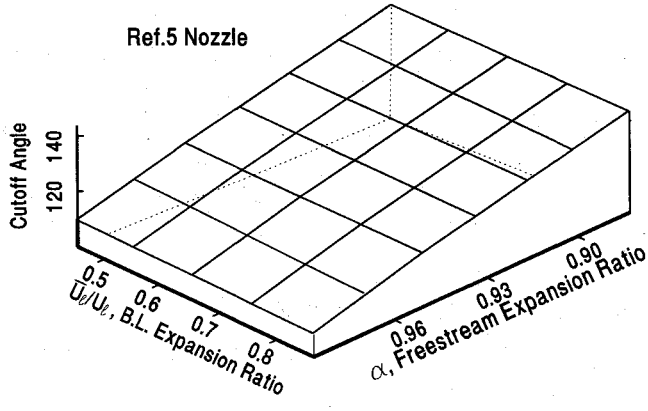

Fig. 4 General solution surface for Ref. 5 nozzle.

$$f(\theta) = f(\theta_0)\exp[-\beta(\theta - \theta_0)] \qquad \text{for} \qquad \theta_0 \le \theta \le \theta_\infty \tag{3}$$

Flow originates from the isentropic core for angles $\theta \le \theta_0$ and from the boundary layer for angles $\theta_0 < \theta \le \theta_\infty$. Values for K, θ_0, and β must be known before the local density can be determined from Eq. (1). Following Zana and Hoffman,[5] these parameters are given by

$$K = \sqrt{\frac{\gamma+1}{\gamma-1}}\,\frac{\pi^2}{8\,\theta_\infty^2} \tag{4}$$

$$\frac{\theta_0}{\theta_\infty} = \frac{2}{\pi}\cos^{-1}\left\{\left[\left(\frac{2\delta}{R_e}\right) - \left(\frac{\delta}{R_e}\right)^2\right]^{\frac{\gamma-1}{\gamma+1}}\right\} \tag{5}$$

$$\beta^2 - \frac{\sin\theta_0}{C}\beta + \left(1 - \frac{\cos\theta_0}{C}\right) = 0 \tag{6}$$

where

$$C = \frac{1}{2K}\left(\frac{\gamma-1}{\gamma+1}\right)^{1/2}\frac{U_\ell}{\bar{U}_\ell}\left[\left(\frac{2\delta}{R_e}\right) - \left(\frac{\delta}{R_e}\right)^2\right]^{\frac{\gamma-1}{\gamma+1}} \tag{7}$$

Equation (4) results from consideration of the entire plume mass flow, whereas Eqs. (5) and (6) result from consideration of just the boundary-layer mass flow, with second-order terms in δ, the boundary-layer thickness, retained.

Equations (1–7) are not applicable in the transition and free-molecular portions of the plume flowfield. To simplify

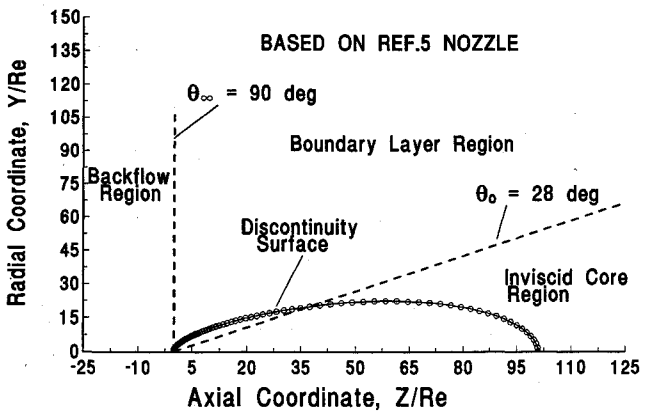

Fig. 5 Discontinuity surface geometry, Ref. 5 nozzle.

the computations, it is somewhat common to reduce the transition zone to a single transition or discontinuity surface, across which the flow passes immediately from continuum to free-molecular behavior. If one defines the discontinuity surface as one of constant Knudsen number K_n, as in Ref. 7, one can readily show that the discontinuity surface for a nozzle with an expansion ratio A_e/A^* is given by

$$\frac{r}{R_e} = \sqrt{\frac{2(\gamma+1)}{\gamma-1}\,\frac{\pi^3 \rho^* N_A d^2 R_e K_n}{8\,\theta_\infty^2 (A_e/A^*) MW}\, f(\theta)} \tag{8}$$

The overall plume structure associated with this model is shown in Fig. 1.

The breakdown of the continuum equations may also be characterized by Bird's parameter[8]:

$$P = \frac{u}{\rho \nu}\left|\frac{\mathrm{d}\rho}{\mathrm{d}s}\right| \tag{9}$$

Using the classical definition of molecular collision frequency and calculating $\mathrm{d}\rho/\mathrm{d}s$ from Eq. (1), one can easily show that Bird's parameter for Simons' flow model is

$$P = \sqrt{\frac{\gamma\pi}{\gamma-1}\,\frac{\alpha^2}{1-\alpha^2}}\, K_n \tag{10}$$

where α, the ratio of actual flow velocity to the adiabatic limiting velocity, is assumed to be constant. Thus, for the present case, constant K_n surfaces are also surfaces of constant Bird's parameter P.

On the constant K_n (P) surface, the gas is assumed Maxwellian with a mean velocity $u = \alpha U_\ell$ in the radial direction. Following Noller[6] and, later, Grier,[7] the number density $\mathrm{d}n_p$ at a point $p(x, y, z)$ due to molecules leaving an elemental volume $\mathrm{d}\tau$ adjacent to the discontinuity surface is given by

$$\mathrm{d}n_p = n_\tau \pi^{-3/2} e^{-\bar{u}^2}\{\tfrac{1}{2}\,\bar{u}\cos\psi + (\tfrac{1}{2} + \bar{u}^2\cos^2\Psi) e^{\bar{u}^2\cos^2\psi}\,\frac{\sqrt{\pi}}{2}\,[1 + \mathrm{erf}\,(\bar{u}\cos\psi)]\}\,\mathrm{d}\Omega \tag{11}$$

The appropriate geometry is illustrated in Fig. 2. Now

$$\cos\psi = \frac{\bar{L}}{|\bar{L}|}\cdot\hat{r} \tag{12}$$

and

$$\mathrm{d}\Omega = \frac{\bar{L}\cdot\hat{n}\,\mathrm{d}\sigma}{|\bar{L}^3|} \tag{13}$$

The coordinates for the elemental volume $\mathrm{d}\tau$ are (r, θ, ϕ) and the coordinates for an arbitrary point in space outside the discontinuity surface are (x, y, z). One can show that

$$\cos\psi = \frac{z\cos\theta + y\sin\theta\cos\phi - r}{|\bar{L}|} \tag{14}$$

and

$$\bar{L}\cdot n\,\mathrm{d}\sigma = [y\cos\phi(\sin\theta + \beta\cos\theta) + z(\cos\theta - \beta\sin\theta) - r]r^2\sin\theta\,\mathrm{d}\theta\,\mathrm{d}\phi \tag{15}$$

for $\theta_0 \le \theta \le \theta_\infty$, and

$$\bar{L}\cdot\hat{n}\mathrm{d}r = \left\{y\cos\phi\left[\sin\theta + \frac{\pi}{2\theta_\infty}\tan\left(\frac{\pi\theta}{2\theta_\infty}\right)\cos\theta\right] + z\left[\cos\theta - \frac{\pi}{2\theta_\infty}\tan\left(\frac{\pi\theta}{2\theta_\infty}\right)\sin\theta\right] - r\right\} r^2\sin\theta\,\mathrm{d}\theta\,\mathrm{d}\phi \tag{16}$$

for $0 \le \theta \le \theta_0$. In both regimes, the line of sight distance is

$$|\bar{L}| = (y^2 + z^2 + r^2 - 2yr\sin\theta\cos\phi - 2rz\cos\theta)^{1/2} \tag{17}$$

Finally, using Eq. (1), one can express the number density n_τ as

$$n_\tau = \frac{N_A \rho^* K f(\theta)}{MW(A_e/A^*)(r/R_e)^2} \tag{18}$$

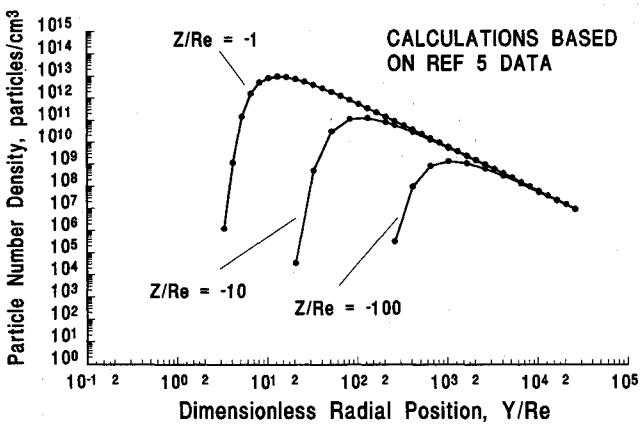

Fig. 6 Particle number density distributions for Ref. 5 nozzle geometry, z = const.

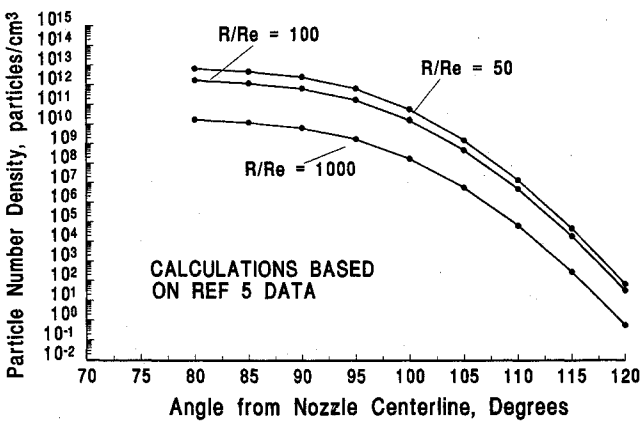

Fig. 7 Particle number density distributions for Ref. 5 nozzle geometry, $R = z^2 + y^2$ = const.

The total number density at $p(x, y, z)$ is obtained by integration as

$$n_p = \int_{\theta=0}^{\theta=\theta_\infty} \int_{\phi=-\pi/2}^{\phi=\pi/2} dn_p \qquad (19)$$

Of course, only portions of the discontinuity surface that are directly visible from $p(x, y, z)$ contribute to the total.

Results

Examination of the model equations indicates that there are three somewhat arbitrary parameters included in the analysis: α, the ratio of actual streamline velocity to the theoretical limiting velocity; $\bar{U}_\ell/U_\ell$, the ratio of the average velocity in the boundary layer to the theoretical limiting velocity; and the parameter P (or K_n) for the discontinuity surface. These parameters fall within the following ranges:

$$\sqrt{\frac{(\gamma-1)M_e^2}{2+(\gamma-1)M_e^2}} \le \alpha \le 1.0$$

(where the lower limit represents no further expansion of the flow outside the nozzle and corresponds to u/U_ℓ at the nozzle exit Mach number M_e);

$$\sqrt{\frac{\gamma-1}{\gamma+1}} < \bar{U}_\ell/U_\ell < \alpha$$

(where $\bar{U}_\ell/U_\ell$ is restricted to supersonic flow in the boundary layer at the lower value and by freestream velocity at the upper value);

$$0.05 \le P \le 2.0$$

(these values represent commonly accepted values for the onset of transition flow and of free-molecular flow, respectively).

It should be noted that the flow is assumed to expand to its theoretical limiting angle, regardless of the value of the velocity ratio α.

Zana and Hoffman[5] have experimentally investigated the exhaust plume of a 90:1 area ratio resistojet thruster using CO_2 propellant. An interesting feature of the overall flow is the large portion occupied by the wall boundary layers. Included in the reported results are a small number of data points in the backflow region in which molecular number density values are measured. Although there appears to be some uncertainty in the quantitative results, the investigators do report a rapid number density falloff at angles larger than about 100 deg, as measured from the nozzle centerline.

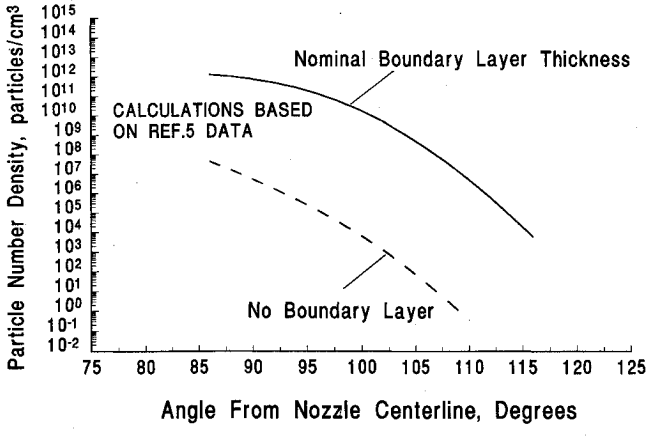

Fig. 8 Effect of nozzle boundary-layer thickness, Ref. 5 nozzle geometry.

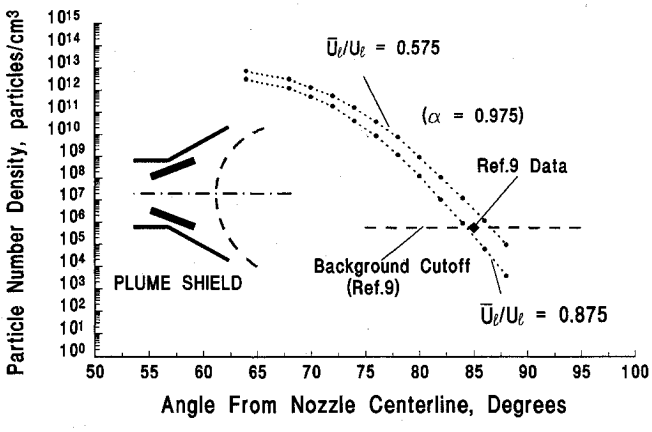

Fig. 9 Plume shield calculations, Ref. 9 nozzle geometry.

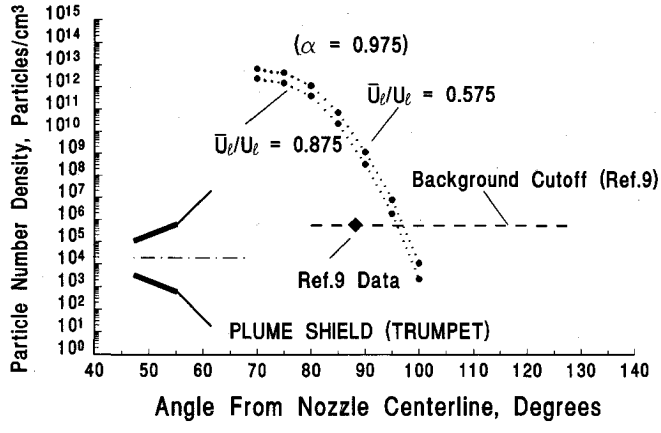

Fig. 10 Trumpet (shield) calculations, Ref. 9 nozzle geometry.

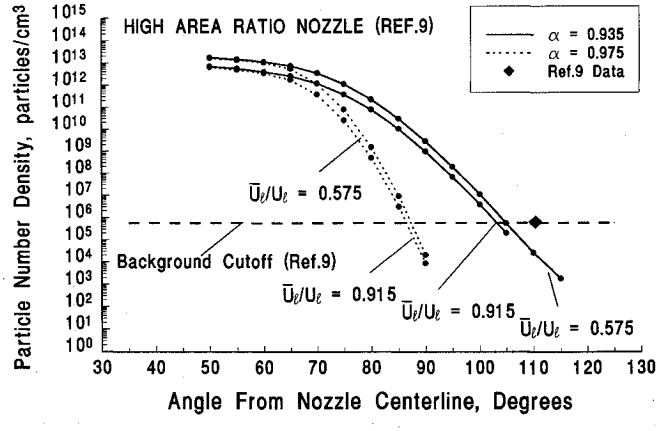

Fig. 11 High area ratio nozzle (Ref. 9) calculations.

Data (nozzle geometry, thermodynamic parameters, etc.) from Ref. 5 were input to the present model in an attempt to predict the reported molecular number densities. Results are shown in Fig. 3. Calculations are performed for two values of α, 0.915 and 0.975, and two values of $\bar{U}_\ell/U_\ell$, 0.575 and 0.875, respectively. Variations with α reflect a dependency on freestream flow expansion, whereas variations of $\bar{U}_\ell/U_\ell$ reflect a dependency on expansion of the supersonic portion of the boundary-layer flow. Measured values reported in Ref. 5 are shown for comparison. The theoretical (continuum) expansion angle is 90 deg for this case. The background cutoff refers to background flux (noise), as reported in Ref. 5.

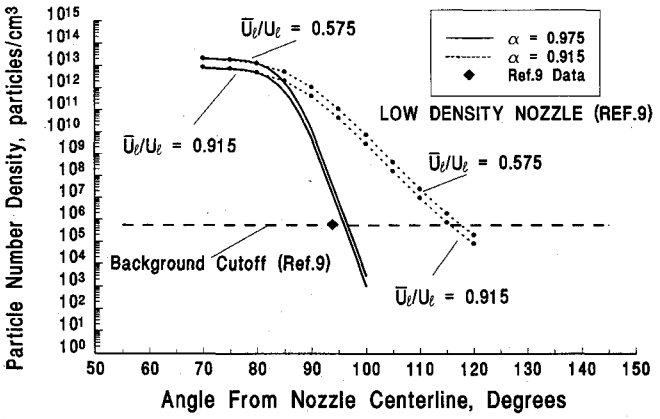

Fig. 12 Low-density nozzle (Ref. 9) calculations.

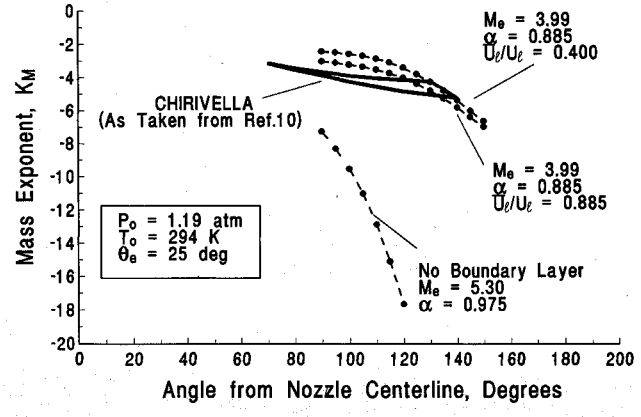

Fig. 13 Mass exponent calculations, 25-deg nozzle (Ref. 10).

More general results are shown in Fig. 4, wherein a solution surface, representing the predicted angle at which the particle number density decreases to the background flux, is plotted vs the parameters α and $\bar{U}_\ell/U_\ell$. All predicted values on the solution surface lie above the measured value[5] of 100 deg for this case.

Figure 5 illustrates a typical discontinuity surface. It should be noted that since $f(\theta)$ does not vanish at $\theta = \theta_\infty$, r/R_e need not vanish at $z = 0$ (the nozzle exit plane). In fact, there is no a priori reason why r/Re should be < 1 at that point. This condition can be satisfied, however, by adjustment of P and $\bar{U}_\ell/U_\ell$.

Figure 6 illustrates the predicted variation in molecular number density in a given axial plane at arbitrary radial distances from the plume centerline. Figure 7 shows the number density variation along a constant radius, with angular position measured from the nozzle centerline. Both cases are for the nozzle conditions of Ref. 5. Finally, Fig. 8 serves to compare the predicted number density distributions for the cases of no boundary layer and a nominal boundary-layer thickness for the nozzle of Ref. 5.

Breyley et al.[9] have investigated the effects of nozzle geometry on the plume structure of a CO_2 resistojet exhausting into a vacuum. One of the nozzle geometries was that of Ref. 5; other configurations included the same nozzle fitted with a "trumpet" extension and the nozzle/trumpet combination fitted with a plume shield. The present simplified analysis cannot readily differentiate the trumpet/plume shield configuration from a shield-only configuration. However, a plume shield can be modeled by assuming that portions of the discontinuity surface at which the line of sight to some arbitrary point in space is blocked do not contribute to the particle number density at that point.

Results for the trumpet/plume shield configuration are shown in Fig. 9. Pertinent nozzle data[9] are identical to that of Ref. 5. For $\alpha = 0.975$, the predicted cutoff points are in reasonable agreement with the 85-deg value reported in Ref. 9. In keeping with the simplicity of the present model, the trumpet configuration of Ref. 9 was treated as a small plume shield located at the exit of the original nozzle (Fig. 4). Results are shown in Fig. 10 and are compared with the 90-deg value reported in Ref. 9.

Also reported in Ref. 9 are results for a high area ratio (900:1) nozzle with the same upstream conditions as those for the previous cases, as well as a low chamber pressure (5×10^{-2} atm) nozzle with an area ratio of 250:1. Calculated number densities for these two cases are shown in Figs. 11 and 12, respectively.

Boraas[10] has developed an analytical model for the backflux, based on the existence of an inviscid cone-shaped continuum region downstream of the nozzle, with molecular flow originating at the surface of the cone. As part of his analysis, and for data comparison purposes, Boraas expresses backflux in terms of flow rate per unit solid angle $(d\dot{m}/d\Omega)_\theta$, normalized by the equivalent value at the nozzle centerline. The resulting equation is a function of the plume shape factor as defined by Hill and Draper[11] and the average thermal velocity of the impinging molecules and can be expressed in terms of a θ-dependent mass exponent K_M as

$$g(\theta) = 10^{K_M(\theta)} \tag{20}$$

One of the computations performed by Boraas is for a 25-deg half-angle conical nozzle with a CO_2 propellant, as used by Chirivella.[12]

It is therefore of interest to calculate the mass exponent for this nozzle with the present model. For the calculations performed, the average thermal velocity of the impinging molecules was approximated by the most probable thermal molecular velocity, which for this analysis is related directly to

Table 1 Summary of results

Nozzle Description	Nozzle exit angle, deg	Continuum limit angle, deg	Isentropic core angle, deg	Background cutoff angle, deg	
				Measured	Calculated
90:1 area ratio, Ref. 5	20	90	28	~100	~107
Shield/trumpet, Ref. 9	20[a]	90	28	~85	~85
Trumpet only, Ref. 9	20[a]	90	28	~90	~95
900:1 area ratio, Ref. 9	10	64	9	~110	~105
Low-density, nozzle, Ref. 9	10	81	6	~95	~97

[a]Neglecting trumpet effect.

the ratio α. Results are shown in Fig. 13. One computation was performed assuming that the wall boundary-layer thickness is negligible, corresponding to a nozzle exit Mach number $M_e = 5.30$, with $\alpha = 0.975$. The molecular number density is greatly underpredicted at all values of θ beyond the limiting flow angle (90 deg). A second computation was performed using a boundary-layer thickness corresponding to $M_e = 3.99$, which is the "data match" Mach number of Ref. 10; for this case $\alpha = 0.885$ and $\bar{U}_\ell/U_\ell = \alpha$. A third computation was made for $\alpha = 0.885$, and $\bar{U}_\ell/U_\ell = 0.40$, which is near the minimum theoretical value for this case. The lower values for α and $\bar{U}_\ell/U_\ell$ are consistent with the lower "effective" expansion ratios associated with the larger boundary layers.

Conclusions

Results of the comparison of model predictions with existing experimental data are summarized in Table 1. Generally speaking, best data matches were achieved by using high particle acceleration parameters (α, $\bar{U}_\ell/U_\ell$) for the relatively low expansion nozzles and low particle acceleration parameters for the high area ratio nozzle, indicating a possible link between nozzle expansion and the plume acceleration parameters.

Typical calculations (e.g., all of Fig. 8) require about 4–6 min on a 386 PC desktop computer. All calculations were made using a 90 (θ direction) $\times$ 30 (ϕ direction) grid. Using a 900×300 grid increased the run times significantly but did not change any calculated particle number density value by more than 0.4%.

It therefore seems that this simple method for calculating particle number density in the backflow region of a nozzle plume expanding into a vacuum may be of some use in obtaining initial estimates and in general parametric studies. Of course, the DSMC method must be used to obtain truly accurate values.

References

[1]Simons, G. A., "Effect of Nozzle Boundary Layers on Rocket Exhaust Plumes," *AIAA Journal,* Vol. 10, No. 11, 1972, pp. 1534, 1535.

[2]Hoffmann, R. J., Kawasaki, A., Trinks, H., Bindemann, I., and Ewering, W., "The CONTAM 3.2 Plume Flowfield Analysis and Contamination Prediction Computer Program: Analysis Model and Experimental Verification," AIAA Paper 85-0928, June 1985.

[3]Bird, G. A., *Molecular Gas Dynamics,* Clarendon Press, Oxford, England, UK, 1976.

[4]Boyd, I. D., and Stark, J. P. W., "Modelling of Small Hydrazine Thruster Plumes Using Discrete Particle and Continuum Methods," AIAA Paper 88-2631, June 1988.

[5]Zana, L. M., and Hoffman, D. J., "An Analytical and Experimental Investigation of Resistojet Plumes," AIAA Paper 87-0399, Jan. 1987.

[6]Noller, H. G., "Approximate Calculation of Expansion of Gas from Nozzles into High Vacuum," *Journal of Vacuum Science Technology,* Vol. 3, No. 4, 1966, pp. 202–207.

[7]Grier, N. T., "Back Flow from Jet Plumes into Vacuum," NASA TN D-4978, Jan. 1969.

[8]Bird, G. A., "Breakdown of Continuum Flow in Freejets and Rocket Plumes," *Rarefied Gas Dynamics,* Vol. 74, Progress in Astronautics and Aeronautics, AIAA, New York, 1981, pp. 681–694.

[9]Breyley, L., Serafini, J. A., Hoffman, D. J., and Zana, L. M., "Effect of Nozzle Geometry on the Resistojet Exhaust Plume," AIAA Paper 87-2121, June 1987.

[10]Boraas, S., "Spacecraft Contamination from Rocket Exhausts," AIAA Paper 81-1385, July 1981.

[11]Hill, J. A. F., and Draper, J. P., "Analytical Approximation for the Flow from a Nozzle into a Vacuum," *Journal of Spacecraft and Rockets,* Vol. 10, No. 10, 1966, pp. 1552–1559.

[12]Chirivella, J. E., "Molecular Flux Measurements in the Back-Flow Regions of a Nozzle Plume," Jet Propulsion Lab., California Inst. of Technology, TM 33-620, Pasadena, CA, July 1973.

James E. Daywitt
Associate Editor